Int. J. Electrochem. Sci., 13 **(2018)** 4535 – 4547, doi: 10.20964/2018.05.56

International Journal of ELECTROCHEMICAL SCIENCE
www.electrochemsci.org

Short Communication

Sensitive Detection of Baicalein Based on GR/DNA/GCE

Ningning Zhang[1], *Xu Zhu*[2,*], *Baoxia Liu*[2], *Zhu Chang*[2], *Yuanqiang Hao*[2], *Yintang Zhang*[2],*Maotian Xu*[2], *Baoxian Ye*[1]

[1] College of Chemistry and Molecular Engineering, Zhengzhou University, Zhengzhou 450001, People's Republic of China
[2] Henan Key Laboratory of Biomolecular Recognition and Sensing, College of Chemistry and Chemical Engineering, Henan Joint International Research Laboratory of Chemo/Biosensing and Early Diagnosis of Major Diseases, Shangqiu Normal University, Shangqiu 476000, People's Republic of China
[*]E-mail: ocina@yeah.net

Received: 15 December 2017 / *Accepted:* 4 March 2018 / *Published:* 10 April 2018

We report herein a sensitive electrochemical assay for the detection of baicalein. The highly-active working electrode was obtained by decorating the glassy carbon electrode modified with graphene and DNA (GR/DNA/GCE), which was characterized by cyclic voltammetry (CV) and electrochemical impedance spectroscopy (EIS). Electrochemical behavior of baicalein on the (GR/DNA/GCE) was systematically studies. Under optimized conditions, the typical oxidation current was found linear with concentration of baicalein in a range of 7.3×10^{-7} ~ 1.17×10^{-4} M with a low detection of 3.2×10^{-7} M.

Keywords: Baicalein, Electrochemical sensor, Graphene, DNA

1. INTRODUCTION

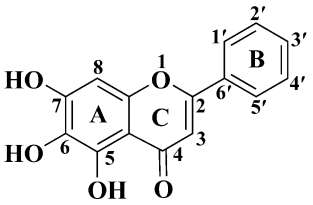

Scheme 1. The structure of baicalein.

Baicalein (BA, 5, 6, 7-trihydroxyflavone, Scheme 1), a kind of natural flavonoids present in *Scutellaria baicalensis*, has attracted considerable attention due to its pharmacological activities such as anti-allergy [1], anti-HIV [2], and anti-tumor [3, 4]. Furthermore, it has been found that BA would be a potential drug in preventing and treating both Alzheimer disease [5] and Parkinson disease [6] owing to its antioxidation properties. Due to these significant phytopharmaceutical usages, it is very important to develop fast and robust tool for the quantitative detection of baicalein.

So far, several chromatographic techniques have been proposed for the detection of baicalein, including capillary electrophoresis (CE) [7], gas chromatography (GC) [8], thin layer chromatography (TLC) [8], reversed phase high performance liquid chromatography (RP-HPLC) [9, 10], HPLC coupled to mass spectrometry (HPLC-MS) [11], and attenuated-total-reflectance infrared (ATR-IR) [12]. Although these methods have obtained high sensitivities and resolutions, there are some shortcomings need to be addressed, such as their complicated handling procedures and requirements of intricate equipments.

Alternatively, electrochemical methods have received a great deal of attention due to its advantages of simplicity, high sensitivity, good selectivity and reliability, rapid response and low cost. Moreover, BA is highly electrochemical active ascribed to its aromatic hydroxyl groups. Previous studies on the electrochemical behavior of BA have shown that BA exhibited three oxidation peaks at 0.09 V, 0.53 V and 0.83 V and one reduction peak at 0.07 V (*vs*. Ag /AgCl) in phosphate buffer (pH 7.0) [13]. It was suggested that the three oxidation peaks in proper order from low potential to high one were corresponding to the oxidation of 6,7-hydroxyl groups, 5-hydroxyl group on A-ring and the further oxidation of the redox product of A-ring, respectively, and the reduction peak was from the reduction of the oxidation product of 6,7-hydroxyl groups on A-ring. On the basis of the redox properties of BA, several electrochemical assays have been developed for its detection based on various modified electrodes [14-18].

Graphene has received a growing research interest in recent years. Considering its excellent electroconductivity, high electron mobility properties along with its exceptionally large surface area, graphene is expected to be an attractive material for electrochemical sensorand has also been used in many sensing strategies to achieve target detection with high sensitivity [19, 20]. Extensive researches have been used on DNA-modified electrodes as an electrochemical sensor to small molecules [21, 22].

Inspired by these above-mentioned studies, we reported herein a sensitive electrochemical assay for the detection of BA based on a GR/DNA/GCE. Cyclic voltammetric behavior of BA on GR/DNA/GCE was studied, and the influence of electrolytes, pH, and scanning rate were also inspected. The cyclic voltammogram displayed two oxidation peaks at 0.140 V and 0.607 V, respectively. Under optimized conditions, the oxidation current at 0.140 V was successfully exploited for the quantitative determination of BA with a dynamic range of 7.3×10^{-7} ~ 1.17×10^{-4} M and a low detection of 3.2×10^{-7} M. The proposed electrochemical assay also displayed high specificity for BA over other interferences.

2. EXPERIMENTAL

2.1 Chemicals and reagents

A 2.2 mmol·L^{-1} stock standard solution of BA (purity >95%， Panya Chemical Co. Ltd. Shanghai, China) was prepared in ethanol solution and was stored at 4 ^{o}C. The working standard solutions of BA were prepared by diluting the stock solution with buffer solution before use. Graphite powder (Beijing Chemical Reagent Factory, Beijing, China). BR, HAc-NAc, Tris-HCl at pH 7.0 and a series of phosphate buffer solution (PBS) with different pH values and were prepared. All chemicals were of analytical-reagent grade. Twice distilled water was used throughout.

2.2 Preparation of graphene oxide

Hummer's graphene oxide was synthesized following literature procedure. Typically, 1.0 g of graphite powder, 0.5 g $NaNO_3$ and 23 mL H_2SO_4 (dense) was added in a beaker placed in an ice bath to maintain the temperature below 10 ^{o}C. $KMnO_4$ (3 g) was slowly added into it with constantly stirring. The suspension was transferred into a 40 °C water bath and further stirred for 40 min followed by the slowly addition of 46 mL of Milli-Q water and the temperature was raised to 90 ± 5 ^{o}C for 20 min with continuous stirring. Finally, 75 mL of Milli-Q water was added followed by the titration of 3.0 mL of H_2O_2 (30%) until the colour of the solution changed from dark brown to yellow. The resulting solution was centrifuged and the residue was washed with Milli-Q water for several times followed by the centrifugation until the pH of supernatant approximate 7.0. Finally the residue was ultrasonic disperse in solution.

2.3 Electrode Preparation

Before modification, glassy carbon electrode (GCE) (3 mm diameter) was polished to a mirror-like surface with 0.03 μm Al_2O_3 slurry, and washed thoroughly with Milli-Q water. Subsequently, a 4.0 μL suspension of graphene oxide (GO) and DNA was scrupulously dropped onto the surface of the polished electrode and dried under an infared lamp, obtaining GCE modified with GO and DNA (GO/DNA/GCE). Afterwards, the GO/DNA/GCE was put into PBS(pH 7.0, 0.1 M) for cyclic voltammograms scanning 8 cycles in a potential range from 0.0 to 1.8 V to get GR/DNA/GCE. After that, the surface of GR/DNA/GCE rinsed by Milli-Q water carefully. For comparison, glassy carbon electrode modified with DNA (DNA/GCE) and glassy carbon electrodmodified with grapheme (GR/GCE) were prepared in a similar procedure.

2.4 Detection of BA

For investigate oxidation behavior of BA, 5 mL PBS (pH 7.0) buffer containing an appropriate BA was transferred into a voltammetric cell. The cyclic voltammograms of BA were recorded in the potential range of -0.3 ~ 0.9 V at 0.05 V·s^{-1}.

2.5 Real sample assay

Sculellaria barbata and Huang-Qin was purchased from a local pharmacy in Shangqiu. Firstly, the leaf of sculellaria barbata and the stem of Huang-Qin were finely powdered in an agate mortar; secondly, accurate amount of the powder was weighed and extracted with 10 mL ethanol for 30 minutes in an ultrasonic bath; finally, the supernatant was gathered by centrifuged. The above there steps were repeated for five times, and all the extraction solution was merged and evaporated to a certain volume for analysis. The sample was stored at 4 °C in the dark. Prior to each measurement, the sample solution was diluted quantitatively with 0.1 M PBS (pH 7).

3. RESULTS AND DISCUSSION

3.1 Electrochemical Characteristics of the GR/DNA/GCE

The electrochemical characteristics of different electrodes, including GCE, GR/GCE, DNA/GCE and GR/DNA/GCE was investigated by CV in 1.0×10^{-3} M $K_3[Fe(CN)_6]$ containing 0.1M KCl and the results are presented in Figure 1A. For the GCE, a pair of reversible redox peaks was obtained with an I_{pa} of 16.05 μA and I_{pc} of 15.88 μA. The redox currents were noticeably decreased at the GR/GCE and DNA/GCE, which might be due to that casting GR and DNA changed the interface state of the GCE. On the other hand, compared with GCE, the current of GR/DNA/GCE was also decreased, and the I_{pa} currents decreased to 13.99 μA and I_{pc} of 14.53 μA, while the charge current was increased, indicating an even larger surface area for the GR/DNA modified membrane and increased electrostatic repulsion between negatively charged GR and $Fe(CN)_6^{3-/4-}$. This also proved that GR/DNA was modified on the electrode successfully[23,24].

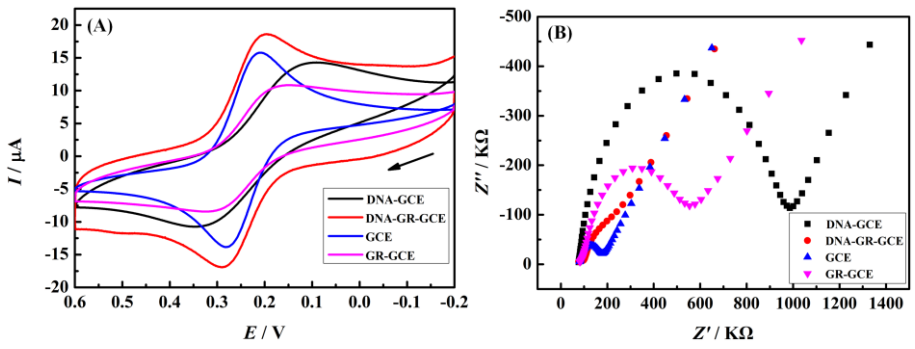

Figure 1. (A) CV curves at GCE, GR/GCE, DNA/GCE and GR/DNA/GCE in 1.0×10^{-3} M $K_3[Fe(CN)_6]$ containing 0.1M KCl, Scan rate, 0.05 V s^{-1}. (B) Nyquist plots of EIS at GCE, GR/GCE, DNA/GCE and GR/DNA/GCE in 1.0×10^{-2} M $[Fe(CN)_6]^{3-/4-}$ containing 0.1 mol L^{-1} KCl.

EIS is important for clarifying the electrochemical performance of an electrode. Nyquist plots of the bare GCE, DNA/GCE, GR/GCE and GR/DNA/GCE were recorded in 1×10^{-2} M $[Fe(CN)_6]^{3-/4-}$ containing 0.1 mol L^{-1} KCl as supporting electrolyte (1×10^{-2} Hz to 1×10^{5} Hz) (Figure 1B). The semicircle diameter obtained at higher frequency (on the Nyquist plot) corresponds to the electron-

transfer resistance (R_{et}) [25]. The linear portion at lower frequency might be attributed to the diffusion-limited process. Compared with GCE (112 Ω), the R_{et} value of GR/GCE (364 Ω) and DNA/GCE (783 Ω) increased considerably ascribed to the increasing electrostatic repulsion between negatively charged GR with DNA and $Fe(CN)_6^{3-/4-}$ which hindered the interfacial charge-transfer. When GR/DNA membrane was coated on the surface of GCE , the R_{et} value (245 Ω) decreased significantly.

3.2 Cyclic voltammetric behavior of BA at different modified electrodes

The electrocatalytic oxidation of BA at bare and different modified electrodes has been investigated by CV. Figure 2 depicts the cyclic voltammograms of BA on the GCE, GR/GCE, DNA/GCE and GR/DNA/GCE in PBS containing 7.92×10^{-5} M BA. With GCE, the electrochemical response for BA was very weak. The oxidation currents of BA on DNA/GCE were even lower than that of GCE, which might be the tight absorbance of DNA on the electrode surface, and that is not charge conducive. For the GR/GCE, redox peak currents are noticeably increased but less than that on the GR/DNA/GCE. GR/GCE and GR/DNA/GCE appear another reduction peak, which is almost immeasurable at the GCE. For GR/DNA/GCE, self-assembly of DNA onto graphene, the double helix of loose DNA facilitates the immobilization of small molecules such as BA. Thus, it is expectable that a sensitive electrochemical sensor for BA determination would be achieved based on the GR/DNA/GCE.

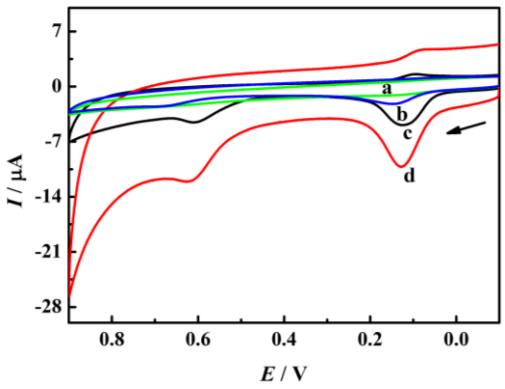

Figure 2. Cyclic voltammograms of BA on DNA/GCE (curve a), GCE (curve b), GR/GCE (curve c) and GR/DNA/GCE (curve d) in PBS (pH 7.0) with scan rate of 0.05 $V\cdot s^{-1}$.

3.3 Optimization of parameters

3.3.1 Influence of the mass ratio of GO and DNA and the amount of GO-DNA composite

The voltammetric response of BA is affected by the mass ratio of GO and DNA, as well as the amount of GR/DNA composite (Figure 3). When extending the mass ratio from 0.054 to 0.1512, the oxidation peak currents gradually increased. However, the oxidation peak currents is reduced at mass ratio range from 0.1512 to 0.216. Considering sensitivity, the mass ratio of 0.1512 (GO : DNA) was selected as the optimum. Figure 3B depicts the influence of the amount of composite on the oxidation

peak currents of BA at the GR/DNA/GCE. when the amount of composite drops is equal to 4 μL, the oxidation peak peaks for BA reaches the maximum.

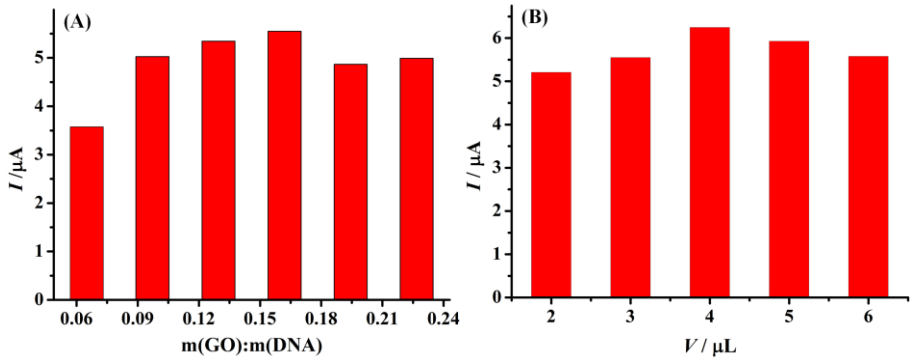

Figure 3. Dependence of I_{pa1} on mass ratio of GO and DNA (A), and the amount of GR-DNA composite (B) in PBS (pH 7.0) with scan rate of 0.05 V·s^{-1}.

3.3.2 Influence of supporting electrolytes and pH

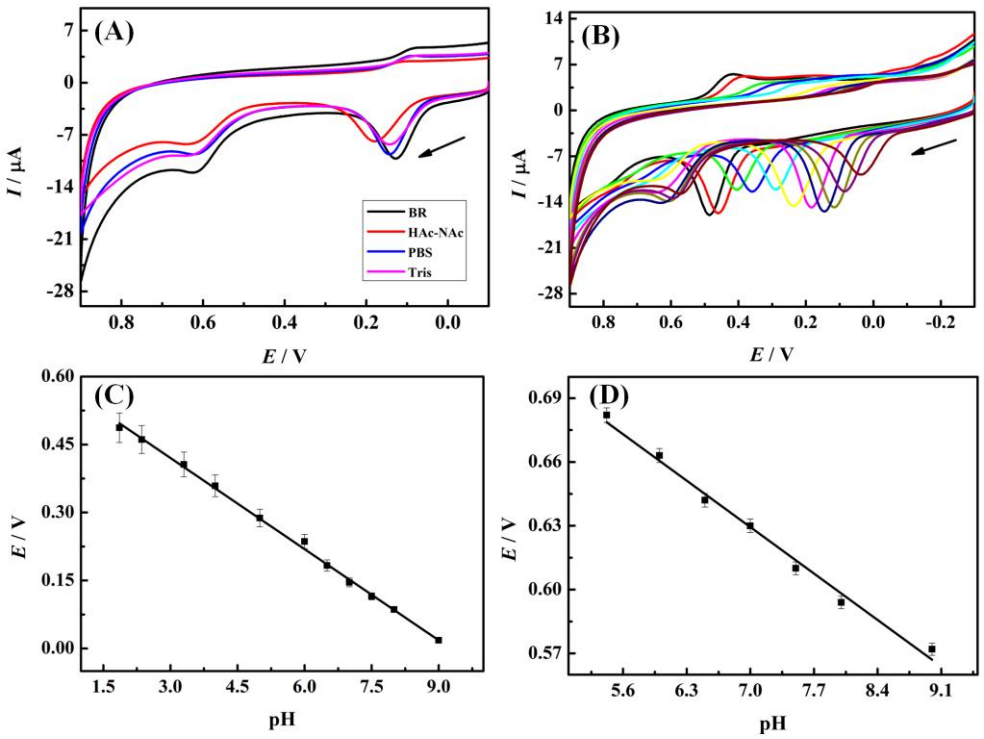

Figure 4. Cyclic voltammograms of BA (7.92×10^{-5} M) at the GR/DNA/GCE with different supporting electrolytes (A) and different pH of PBS from right to left: 9, 8, 7.5, 7, 6.5, 6, 5, 4, 3.3, 2.36, 1.86 (B) with scan rate of 0.05 V·s^{-1}. The relationship between pH with E_{pa1}(C) and E_{pa2} (D).The error bars represent standard deviations for three tests.

To further investigate the effect of supporting electrolytes on the voltammetric response of BA. The impact of different supporting electrolytes, including PBS, BR, Tris-HCl and HAc-NaAc, ware inspected in the presence of 7.92×10^{-5} M BA (Figure 4). These results proved that the best peak current and peak shape were get in PBS. Therefore, PBS was used as the electrolyte in subsequent experiments.

In most case, the pH of supporting electrolytes was an important influence factor to electrochemical reaction. The electrochemical behavior of BA (7.92×10^{-5} M) was investigated at different pH values in the range of 1.86~9.00, the recorded voltammograms for each pH are depicted in Figure 4B. For peak E_{pa1}, pH was below 2.36, the peak current I_{pa1} increased with the decrease of pH value. When pH value was above 2.36, the peak current I_{pa1} increased with the increase of pH value. the peak current I_{pa1} reached to maximum value at pH 7.0. While the I_{pa1} gradually decreased in the range of 7.0~9.0. Moreover, for peak E_{pa2}, the peak current I_{pa2} increased with the increase of pH value when pH value was above 6, and I_{pa1} nearly disappeared in the pH range from1.86 to 6.0. The two oxidation peak potentials for BA negatively shifted with increasing pH values, manifesting that the protons have taken part in their electrode reaction processes. The linear regression equations were E_{pa1} / V = 0.62161-0.06707 pH (R = 0.999) (Figure 4C), E_{pa2} / V = 0.84764-0.03118 pH (R = 0.995) (Figure 4C), respectively. The slope -67.07 mV/pH of E_{pa1}-pH relationship indicated that the proton number was equal to the electron transfer number for peak E_{pa1}, and the slope -31.18 mV/pH of E_{pa2}-pH relationship indicated that the proton number was one half of the electron transfer number for peak E_{pa2}.

3.3.3 Influence of accumulation time and scan rate *v*

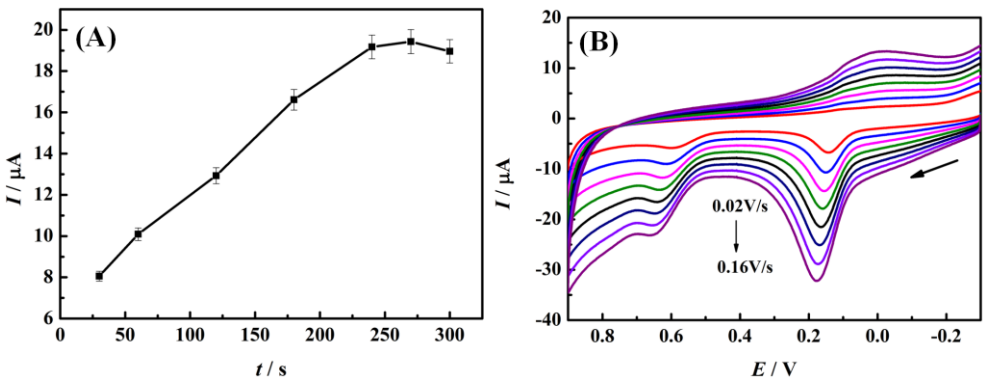

Figure 5. The relationship between I_{pa1} and accumulation time. The error bars represent standard deviations for three tests. (B) CVs of BA (7.92×10^{-5} M) at the GR/DNA/GCE in 0.1 M PBS (pH 7.0) at different scan rates from top to bottom：0.02， 0.04, 0.06，0.08, 0.10，0.12, 0.14，0.16V/s.

Considering that the electrode process may be predominantly controlled by adsorption, an process of accumulation is advantageous to increase the sensitivity of detection. A suitable accumulation time was necessary for the detection, which was performed in a 7.92×10^{-5} M BA solution. Figure. 5A shows the relationship between accumulation time and peak currents. By

extending the accumulation time, the oxidation peak current of I_{pa1} increased up to an accumulation time of 270 s and then maintained stability. Based on the above investigation, an accumulation time of 270 s under open circuit was selected as the condition for detection of BA.

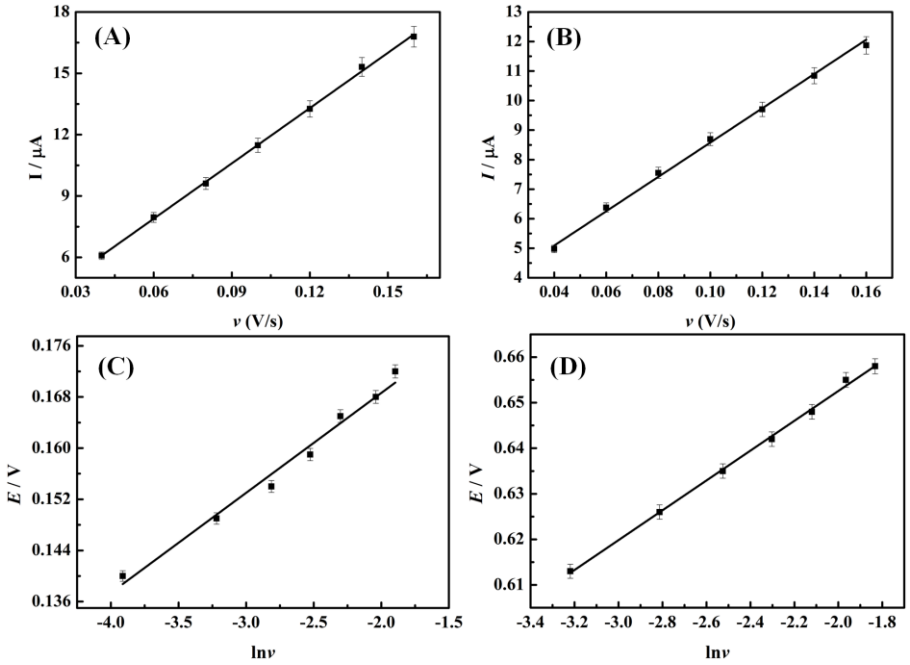

Figure 6. The relationship between I_{pa1} (A) and I_{pa2} (B) with v. The relationship between E_{pa1} (C) and E_{pa2} (D) with ln$v$. The error bars represent standard deviations for three tests.

The effects of scan rate v on both peak current of I_{pa1} and peak I_{pa2} were examined in the scan rate range of 0.02~0.16V·s^{-1} in PBS (pH 7.0) (Figure 5). The peak current I_{pa1} and I_{pa2} is linearly proportional to the scan rate in the range 0.04~0.16V·s^{-1} with the equation: I_{pa1} = 2.48521 + 90.11063 v (V·s^{-1}) (R=0.999) (Figure 6A), I_{pa2} = 2.76969 + 58.07973 v(V·s^{-1}) (Figure 6B), suggesting that the electrochemical process of BA was adsorption-controlled. In addition, the linear relation between E_{pa} (V) and ln$v$(V·s^{-1}) corresponded to the following equation: E_{pa1} (V) =0.019987 ln$v$(V·s^{-1}) + 0.1562 (R = 0.993) (Figure 6C), E_{pa2} (V) =0.03274 ln$v$(V·s^{-1}) + 0.71805 (R = 0.999) (Figure 6D). According to *equation (1)*, proton number n1 and n2 was calculated to 2 and 1, respectively. The E_{pa1} corresponded to a two-electron and two-proton process, while E_{pa2} corresponded to a one-electron and one-proton process.

$$E_{pc}(\mathrm{V}) = E^{0'} - \frac{RT}{\alpha nF}\ln v \qquad (1)$$

3.4 Cyclic Voltammetric behavior of BA at GR/DNA/GCE

The cyclic voltammograms of 7.92×10^{-5} M BA at GR/DNA/GCE in BR (pH 7.0) buffer were showed in Figure 7A. Two well-defined oxidation peaks, E_{pa1} = 0.140 V and E_{pa2} = 0.607 V, appeared

on anodic scan from -0.3 V to 0.9 V and a reduction peak with E_{pc1} 0.076 V appeared on reversal scan. The oxidation peak currents I_{pa1} and I_{pa2} were 11.64 μA and 9.459 μA, respectively. The reduction peak current I_{pc1} was 1.157 μA. Here, it was necessary to check the origin of peak P_{c1}. For this, the cyclic voltammetric behavior of BA was examined further in the potential range of -0.30~0.40 V to avoid the occurrence of peak P_{a2}.

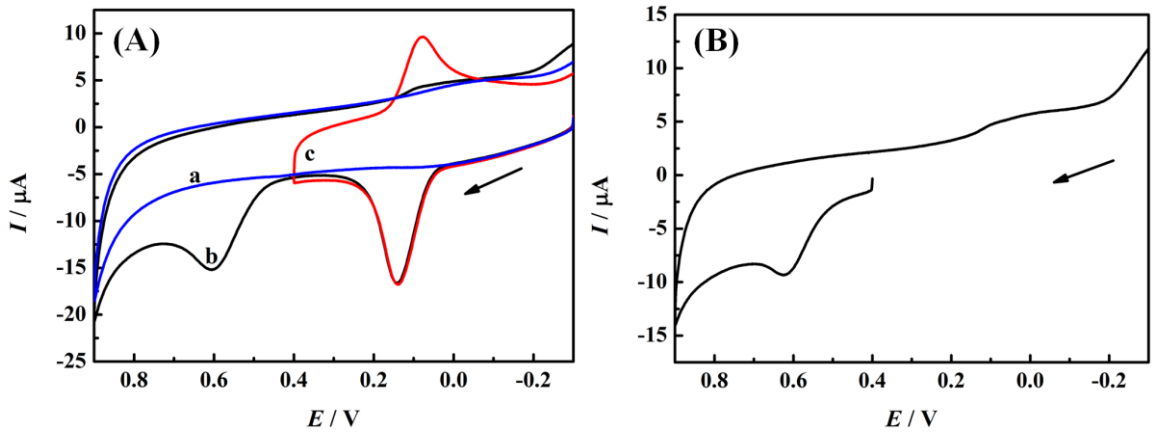

Figure 7. Cyclic voltammograms of 7.92×10^{-5} M BA in PBS (pH 7.0) at different potential range with scan rate of 0.05 $V\cdot s^{-1}$.

That is, the high potential was controlled at 0.40 V that was after peak P_{a1} and before peak P_{a2}. Experiments showed that peak P_{a1} still appeared on anodic scan and peak P_{c1} appeared on reversal scan as well. Moreover, all the peak potentials E_{pa1} and E_{pc1} and the peak current I_{pa1} were the same as those in the potential range of -0.30~0.90 V, and the peak potential separation ΔE_p (E_{pa1} - E_{pc1}) of peak P_{a1} and peak P_{c1} was 64 mV. However, the peak current I_{pc1} of peak P_{c1} increased to 7.069 μA, the peak current ratio I_{pa1} / I_{pc1} of I_{pa1} with I_{pc1} was reduced from about 10 (11.64/1.157) to 1.6 (11.64/7.069).

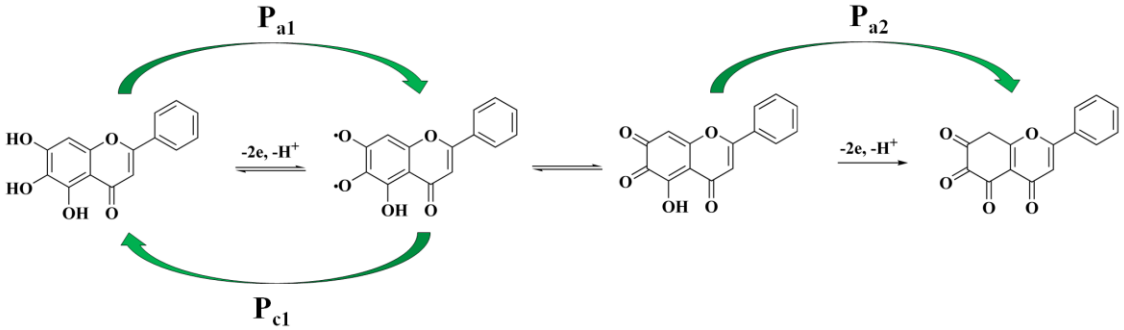

Scheme 2. The proposed redox mechanism of baicalein at GR/DNA/GCE.

These results demonstrated that (1) both peak P_{c1} and peak P_{a1} were from a reversible redox couple. And peak P_{c1} resulted from the reduction of the oxidation product from peak P_{a1}; (2) the fact that the oxidation peak current I_{pa1} was always bigger than the corresponding reduction peak current I_{pc1} in the potential range of either -0.3~0.4 V or -0.3~0.9 V and when the cyclic voltammetric behavior of BA was examined from 0.4 V, the P_{a2} still appeared and I_{pa2} decreased to 5.387 μA (Figure

7B), which foreshowed that P_{a2} is product of another electroactive group, and the reaction Pa1is advantageous to the reaction P_{a2}.

According to previous report[26] and electrochemical knowledge, it was known that *o*-dihydroxyl groups of benzene ring were much easily oxidized (Scheme 2). For BA, the oxidation of 6, 7-dihydroxyl groups on A-ring was easier than that of 5-hydroxyl group, as the latter formed hydrogen bond with the carbonyl group at C_4. Based on the parameters of electrode processes of peak P_{a1} and peak P_{a2} mentioned above and the chemical structure of BA, it could be deduced that BA was oxidized to its *o*-biquinone derivative through a two-electron transfer of 6, 7-dihydroxyl groups on A-ring via an intermediate free radical at lower potential, producing a pair of redox peaks peak P_{a1} and peak P_{c1}. And the fact that the reduction peak current I_{pc1} was smaller than the oxidation peak current I_{pa1} might result from the disproportion of the intermediate free radical. Moreover, the formed BA *o*-biquinone derivative was oxidized to its quinone derivative through a two-electron transfer of 5-hydroxyl group on A-ring at higher potential subsequently, producing peak P_{a2}. Both the oxidation processes of BA were described in Scheme 2.

3.5 Analytical performances of the electrochemical assay for BA

3.5.1 Dynamic range and detection limit

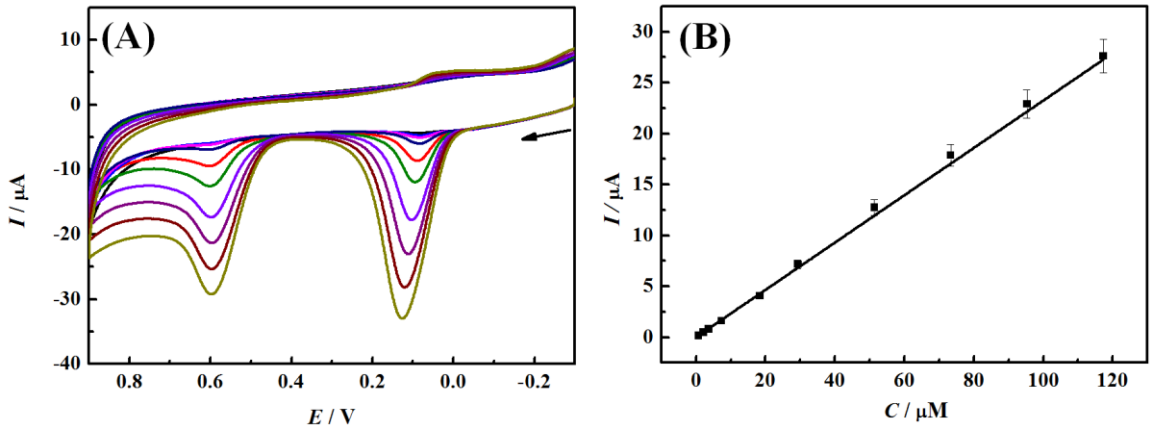

Figure 8 (A) Cyclic voltammograms for different concentration of (7.3×10^{-7} ~ 1.17×10^{-4} M) baicalein in 0.1 M PBS (pH 7.4). (B) The corresponding calibration plot I_p–C. The error bars represent standard deviations for three tests.

Based on the selected optimum conditions, the GR/DNA/GCE based electrochemical assay was proposed for the determination of BA employing CV. For adsorption accumulation, a open circuit technique was selected to attain maximal peak current. The results showed that CV was a suitable technique. Figure 8A shows superimposed CV curves for BA at various concentrations in the 0.1 M PBS (pH 7.0) solution. As shown in the inset, the oxidation currents linearly increased when concentrations of BA were in the range of 7.3×10^{-7} to 1.17×10^{-4} M. The linear regression equation was

expressed as I_{pa1}(A)=0.2327*C* (μM) + 0.01573 (*R* = 0.998). The LOD was calculated as 3.2×10^{-7} M based on an S/N of 3. In addition, the analytical performance of the GR/DNA/GCE was compared with the previous work in Table 1. The standard curve of this work was established by cyclic voltammetry, the sensitivity and detection limits of which are lower than some of other methods, such as, differential pulse voltammetry, square wave anodic stripping voltammograms, etc. Although the detection limit of the present work is higher than previous works, this method can be well applied to the detection and analysis of BA in traditional Chinese medicine. Besides, the developed strategy only need simple operation, cheap materials and easy to control.

3.5.2 Selectivity, reproducibility and stability

For the practical application of the proposed method, some possible co-existing species were investigated in baicalein solution (1.1×10^{-5}M) by CV. The tolerance limit for the interfering species was defined as the maximum concentration that caused a relative error less than ± 5.0%. 50-fold of Zn^{2+}, Fe^{3+}, Cl^{-} , SO_4^{2-}, D-glucose, D-fructose, sucrose, tartaric acid, citric acid, 10-fold of Ca^{2+}, Cu^{2+} did not show any interference. The reproducibility and stability of the GR/DNA/GCE was studied by the measurement of the response to 1.1×10^{-5}M BA in 0.1 M PBS by CV. The relative standard deviation (RSD) of reproducibility for five parallel GR/DNA/GCE in a 1.1×10^{-5}M baicalein was 3.54%, indicating that the quality of the fabrication sensor was at an acceptable level. For testing the stability of the developed sensor, the prepered GR/DNA/GCE was stored in refrigerator at 4 ^{o}C, then was taken out to detect baicalein every week. 90.2% of the initial current signal was obtained, indicating the good long-term stability of the as-expected sensor. Therefore, the proposed method can be used as a selective method.

Table 1. Comparison of the linear ranges and LOD of the different BA sensors

Electrode	Modifier	technology	LOD(μM)	Linear range(μM)	Reference
DE	Boron	LSVs	0.26	1-95	[26]
GCE	Poly-L-lysine	DPV	0.048	0.5-10	[27]
GCE	ErGONRs	AdsDPV	0.12	0.4-50	[28]
CPE	Ta_2O_5-Nb_2O_5@CTS	DPV	0.05	0.08-8.0	[16]
CPE	Ta_2O_5-CTS	LSVs	0.05	0.08-4.0	[17]
GCE	DNA-LB film	SWV	0.006	0.01-2	[29]
GCE	ERGO	SWASV	0.002	0.005-0.5	[30]
CPE	CNTs	SWASV	0.0042	0.02-10	[31]
GCE	GR-DNA	CV	0.32	0.73-117	This work

Abbreviations: DE: diamond electrode; CPE: carbon paste electrode; ErGONRs: electrochemically reduced graphene oxide nanoribbons; Ta_2O_5-Nb_2O_5@CTS: tantalum oxide (Ta_2O_5), niobium oxide (Nb_2O_5) particles and antiseptic chitosan; Ta_2O_5-CTS: tantalum oxide (Ta_2O_5) particles and chitosan; LB film: Langmuir–Blodgett film; ERGO: electrochemical reduced graphene oxide; CNTs:carbon nanotubes; DPV: differential pulse voltammetric; LSVs: linear sweep voltammograms; AdsDPV: adsorptive stripping differential pulse voltammetric; SWV: square wave voltammetric; SWASV: Square wave anodic stripping voltammetric

3.5.3 Real sample analysis

For evaluating the applicability of the current method, it was employed to determine baicalein in the two traditional Chinese herbs. After determination the concentration of baicalein, some standard baicalein was added in the two samples respectively and the total concentration of baicalein were determined again to calculate the recovery (Table 2). The baicalein content in Huang-Qin and sculellaria barbata was calculated to be 4.58 $mg \cdot g^{-1}$ and 1.701$mg \cdot g^{-1}$ with recovered ratios in the of 95.79~100.53% and 94.96~106.09%, respectively. The detection results implied that the constructed electrochemical sensor was available for practical application with good accuracy and selectivity. To test the accuracy of proposed method, the same traditional Chinese herbs were analyzed using HPLC. According to the HPLC results, no significant difference were found between them, but the proposed method was simpler and more time-saving than HPLC.

Table 2. Determination of baicalein in chinese traditional herb Huang-Qin and sculellaria barbata samples.

		CV				HPLC	
Original found[a] ($\times10^{-6}$M)	Standard added ($\times10^{-5}$M)	Total found[a] ($\times10^{-5}$M)	R.S.D (%)	Recovery (%)	Content in sample[a] ($\times10^{-4}$M)	Content in sample[a] ($\times10^{-4}$M)	R.S.D[a] (%)
8.08 (sculellaria barbata)			1.9		8.08	8.12	2.4
	1.15	1.90	2.3	94.96			
	2.30	3.12	1.1	106.09			
	3.45	4.25	1.6	98.26			
15.10 (Huang-Qin)			3.4		7.55	7.58	1.8
	1.90	3.33	2.5	95.79			
	3.80	5.24	0.8	100.53			
	5.70	7.12	2.7	98.95			

[a]Average value of three replicate measurements.

4. CONCLUSION

In this paper we developed a sensitive electrochemical assay for the detection of baicalein based on a new GR/DNA/GCE. The fabrication process and the electrochemical characteristics of GR/DNA/GCE were inspected by CV and ESI. The electrochemical behavior of BA on the GR/DNA/GCE was systematically studied. Under optimized conditions, the electrochemical sensor exhibited a dynamic range of 7.3×10^{-7} ~ 1.17×10^{-4} M for BA with a low detection limit of 3.2×10^{-7} M. The proposed electrochemical assay also displayed high specificity for BA over other interferences.

ACKOWLEDGMENTS
This work was financially supported by the Nation Natural Science Foundation of China (Grant Nos. 21305085, U1404215, 21405103, 21405102, 21675109 and 21475084) and Innovation Scientists and Technicians Troop Construction Projects of Henan Province (No: 41).

References

1. B. Q. Li, T. Fu, W.-H. Gong, N. Dunlop, H.-f. Kung, Y. Yan, J. Kang and J. M. Wang, *Immunopharmacology*, 49 (2000) 295-306.
2. J. A. Wu, A. S. Attele, L. Zhang and C.-S. Yuan, *Am. J. Chin. Med*., 29 (2001) 69-81.
3. Y. Matsuzaki, N. Kurokawa, S. Terai, Y. Matsumura, N. Kobayashi and K. Okita, *Jpn. J. Cancer Res.*, 87 (1996) 170-177.
4. D. E. Shieh, L. T. Liu and C. C. Lin, *Anticancer Res*., 20 (2000) 2861-2865.
5. H. J. Heo, D. O. Kim, S. J. Choi, D. H. Shin and C. Y. Lee, *J. Agric. Food. Chem*., 52 (2004) 4128-4132.
6. M. Zhu, S. Rajamani, J. Kaylor, S. Han, F. M. Zhou and A. L. Fink, *J. Biol. Chem.*, 279 (2004) 26846-26857.
7. L. Qi, R. Zhou, Y. F. Wang and Y. C. Zhu, *J. Capillary Electrophor*., 5 (1998) 181-184.
8. M.-C. Lin, M.-J. Tsai and K.-C. Wen, *J. Chromatogr. A*, 830 (1999) 387-395.
9. K.-C. Wen, C.-Y. Huang and F.-L. Lu, *J. Chromatogr. A*, 631 (1993) 241-250.
10. L. Tong, M. Wan, L. Zhang, Y. Zhu, H. Sun and K. Bi, *J. Pharm. Biomed. Anal*., 70 (2012) 6-12.
11. C. R. Horvath, P. A. Martos and P. K. Saxena, *J. Chromatogr. A*, 1062 (2005) 199-207.
12. M. Navarro Escamilla, F. Rodenas Sanz, H. Li, S. A. Schönbichler, B. Yang, G. K. Bonn and C. W. Huck, *Talanta*, 114 (2013) 304-310.
13. M. d. Vestergaard, K. Kerman and E. Tamiya, *Anal. Chim. Acta*, 538 (2005) 273-281.
14. F. Wang, F. Zhao, Y. Zhang, H. Yang and B. Ye, *Talanta*, 84 (2011) 160-168.
15. D. Kuzmanović, D. M. Stanković, D. Manojlović, K. Kalcher and G. Roglić, *Diamond Relat. Mater*., 58 (2015) 35-39.
16. Z. Xie, W. Lu, L. Yang, G. Li and B. Ye, *Talanta*, 170 (2017) 358-368.
17. Z. Xie, G. Li, Y. Fu, M. Sun and B. Ye, *Talanta*, 165 (2017) 553-562.
18. Y. C. Wang, Z. Wei, J. P. Zhang and X. M. Wang, *Int. J. Electrochem. Sci.*, 11 (2016) 8323-8331.
19. K. S. Novoselov, V. I. Fal′ko, L. Colombo, P. R. Gellert, M. G. Schwab and K. Kim, *Nature*, 490 (2012) 192.
20. V. Mani, B. Devadas and S.-M. Chen, *Biosens. Bioelectron*., 41 (2013) 309-315.
21. K. M. Millan and S. R. Mikkelsen, *Anal. Chem*., 65 (1993) 2317-2323.
22. J. Chen, Z. Liu, H. Peng, Y. Zheng, Z. Lin, A. Liu, W. Chen and X. Lin, *Biosens. Bioelectron*., 98 (2017) 345-349.
23. H.Q.A. Lê, S. Chebil, B. Makrouf, H. Sauriat-Dorizon, B. Mandrand, H. Korri- Youssoufi, *Talanta*, 81 (2010) 1250-1257.
24. A. Miodek, G. Castillo, T. Hianik, H. Korri-Youssoufi, *Anal. Chem.*, 85 (2013) 7704-7712.
25. J.E.B. Randles, *Discuss. Faraday. Soc.*, 1 (1947) 11-19.
26. D. Kuzmanović, D. M. Stanković, D. Manojlović, K. Kalcher and G. Roglić, *Diamond Relat. Mater*., 58 (2015) 35-39
27. B,Yang, F. D. Hu, J. P. Wei, C. M. Wang, *Acta Chim. Sin.*, 22 (2009) 2585-2591.
28. R. D. Tandel, R. S. Naik, J. Seetharamappa, A. K. Satpati, *Journ. Electrochem. Soc.*, 164 (2017) H818-H827.
29. F. Wang, F. Zhao, Y. Zhang, H. Yang, B. Ye, *Talanta*, 84 (2011) 160-168.
30. Y. W. Wang, Y. J. Wu, C. L. Zhao, F. Wang, *J. Chin. Chem. Soc.*, 61 (2014) 1245–1253.
31. J. Zhou, F. Wang, K. Zhang, G. Song, J. Liu, B. Ye, *Microchim. Acta.*, 178 (2012) 179-186.

© 2018 The Authors. Published by ESG (www.electrochemsci.org). This article is an open access article distributed under the terms and conditions of the Creative Commons Attribution license (http://creativecommons.org/licenses/by/4.0/).